Flame Retardant and Antibacterial Coating on Cotton Fabric by Layer-by-Layer Assembly With Huntite-Hydromagnesite, Ammonium Polyphosphate, Chitosan and Aptes

Nurhan Onar Çamlıbel[1] 0000-0002-2647-4728
Emre Koç[2] 0000-0001-5909-9592

[1] Pamukkale University, Engineering Faculty, Textile Engineering Department, Kinikli Campus, Kinikli, Denizli, Türkiye
[2] Gamateks A.Ş., Denizli, Türkiye

Corresponding Author: Nurhan Onar Camlibel, nonar@pau.edu.tr

ABSTRACT

In this study, it was investigated the coating of cotton fabric with huntite-hydromagnesite (HH) or ammonium polyphosphate (APP) solutions as anionic layer and chitosan solutions and nanosols as cationic layer by layer-by-layer (LBL) assembly to gain flame retardancy and antibacterial properties. Growth bilayer number, drying conditions and anionic layer type (HH or APP) affected the flame retardancy and antibacterial properties of coating with LBL assembly. 17% and 22% reduction in the peak heat release rate and 69% and 87% reduction in total smoke release and 26% and 14% reduction in mass loss rate were observed for fabric samples coated with AP solutions for 15 layers with drying after every dipping process (AP15DE) and fabric samples coated with HH solutions for 15 layers with drying after every dipping process, (H15DE) respectively. Thermogravimetric analysis revealed that the residual chars at 600 oC in air increased. The AP15DE exhibited the antibacterial activity against E. coli and S. aureus while H15DE displayed the antibacterial activity against only S. aureus.

1. INTRODUCTION

Cotton fabric as a type of the most popular natural fibers have been widely used applications in apparel, home textiles, medical textiles, military textiles and industrial textiles due to their excellent properties such as dyeability, hydrophilicity, hygroscopicity, biocompatibility, breathability, comfortableness, warmth retention. However, they suffer from their flammable nature with low oxygen index and ignition temperature, which restricts their application. Meanwhile they ensure living condition for the growth of bacteria due to their hydrophilic and porous surface and affects the health of wearers [1]. Therefore, the manufacture of multifunctional cotton fabrics with antibacterial and flame retardant properties recently attracts great interest.

Huntite ($Mg_3Ca(CO_3)_4$) and hydromagnesite ($Mg_5(CO_3)_4(OH)_2.4H_2O$) mixture as flame retardant agent exhibit the endothermical decomposition between 200 and 400 oC and releases water vapor and/or carbon dioxide, which gives rise to fall down of temperature, the dilution of flammable gases and isolation of flame [2-5]. APP as an acid source would collaborate with fabric with necessity additional carbon source such as chitosan to improve the efficiency. Cationic chitosan in acid solution could be paired with anionic APP solution by LBL assembly. Chitosan with nitrogen content and APP with intumescent nature improve the flame retardacy properties of treated materials [6]. Coatings with silica based nanosols could ensure fire protection by forming inorganic barrier. Silica together with nitrogen-based compounds could catalyze the dehydration and carbonization of substrate and decrease the amount of

combustible gases [7, 8]. HH, APP, chitosan and silica instead of halogenous flame retardants with harmful and toxic effects could be proposed as alternative, sustainable flame retardant agents for cotton fabrics.

Various processes such as plasma, microcapsule and UV-curable flame retardant coatings have been improved and studied by most researchers to decrease the combustibility of cotton and/or to achieve its antibacterial activity. But the physical or chemical processes have caused to more difficulties in their industrial applications and/or environmental pollutions. Recently, LBL assembly technique as environmental friendly, simple and low cost due to being water-based technique were investigated to develop multifunctional cotton fabric in academic area and industrial application. The technique is regularly alternating physical deposition of negatively and positively charged nanoparticles or polyelectrolytes on various substrates such as textile fabric. Various flame retardant and antibacterial coatings were applied to textiles with LBL assembly by means of its multiple performances by combining different molecules.

Nonhalogenated flame retardants containing nitrogen, phosphorus and silicon compounds have been researched widely to develop the flame cotton fabrics [9, 10]. Huntite-hydromagnesite [11], APP [6,12-17], chitosan [6,12-15,20,18-26], silica based materials [12,13,25,27-31] were researched to gain flame retardant or antibacterial properties for various textiles by LBL assembly. There are some reports on multifunctional assembly coatings on textiles with flame retardancy and antimicrobial property [1,30,32-37]. The introducing of huntite-hydromagnesite together with APP, APTES and chitosan as antibacterial and flame retardant agent by LBL assembly has not been reported.

In our study, it was recently investigated characterization and manufacturing of flame retardant and antibacterial cotton fabric via layer-by-layer assembly. Anionic charged huntite-hydromagnesite or ammonium polyphosphate solutions and cationic charged chitosan and silica based nanosols has been prepared and coated with 5, 10 and 15 bilayers, substantially. Phosphorous (APP) or CaO and MgO (HH) and silica (GPTMS and APTES), nitrogen (APP, APTES and chitosan) synergism was researched and compared. The cotton fabrics by LBL assembly were structurally characterized by SEM, elemental analysis and FTIR-ATR. Textile characteristics were determined by add-on value, whiteness, tensile strength, elongation. The flame retardancy and thermal behavior of the cotton fabric treated by LBL were studied by limit oxygen index, vertical flame retardancy, cone calorimetry and thermogravimetric analysis (DTA-TG). The antibacterial activity of the fabrics by treated by LBL were measured by bacterial reduction against E. coli as gram-positive bacteria and S.aureus as gram-negative bacteria.

MATERIAL AND METHOD

2.1 Material

Scoured and bleached cotton fabric (plain weave, 118 g/m², 32 ends/cm, and 22 picks/cm) was used in this research. All chemicals used were of reagent grade. Huntite-hydromagnesite powder (HH, Ultracarb 1250) was supplied from Setas Company, Turkey. Ammonium polyphosphate (APP) were provided by Tecnosintesi SPA, Italy. (3-Amino propyl) triethoxy silane (APTES, Sigma-Aldrich, Germany), (3-Glycidyloxy propyl) trimethoxy silane (GPTMS, Merck KGaA, Germany), chitosan (Mw:50000 Da, the degree of deacetylation: 93.2%, Merck KGaA, Germany), sulphuric acid, glacial acetic acid and sodium hydroxide were used for preparation of solutions in layer by layer coating. GPTMS precursor due to high crosslinking effect to improve coating durability and silica content to develop their flame retardancy and APTES due to silica and ammonium content were utilized to enhance their flame retardancy and antibacterial properties. Tecnosintesi APP is an effective flame retardant with 72.5% of phosphorus content (as P_2O_5), low water solubility and 15 μm of average particle size. The APP is proper for solvent and water based intumescent coatings.

2.2 Method

Nanosol (CA) containing APTES (aq. 5 w/v%) and GPTMS (aq. 1 v/v%), chitosan aq. solution (CC), huntite-hydromagnesite (aq. 1 w/v%) (AH) and ammonium polyphosphate (aq. 0.2 w/v%) (AA) solutions were prepared and their pH values respectively adjusted to 3.4, 3.5 and 11 with sulphuric acid, glacial acetic acid and sodium hydroxide. AH and AA solutions stirred for 1 hour on magnetic stirrer. The fabric samples were first dipped into cationic solution called CA code containing APTES and GPTMS aqueous solutions for 30 min, rinsed (30 sec) and dried an oven at 100 ℃ for 15 min. Then the treated fabrics were dipped into anionic solutions called AH or AA codes containing HH or APP aqueous solutions. The fabric was dipped to each solution during 5 min for first layer and 1 min for later layers, rinsed and dried at 100 ℃ for 15 min. One bilayer (BL) including one cationic and one anionic layer on cotton fabrics was gain in the all assembly cycle process. The first BL was composed of cationic solution containing nanosol (CA code) and anionic solution (AH or AA codes) and the second BL was formed from cationic solution containing chitosan (CC code) and anionic solution (AH or AA codes). The fabric was alternately dipped into anionic and cationic solution until the planned number of bilayers on fabrics was reached [25]. The interactions of cationic and anionic charged chemicals with cellulose were schematically illustrated in Figure 1. Firstly, APTES and GPTMS were reacted with hydroxyl groups on cellulose by hydrolysis and condensation reaction. Then APP, HH and chitosan could be bonded by electrostatical interactions to fabric.
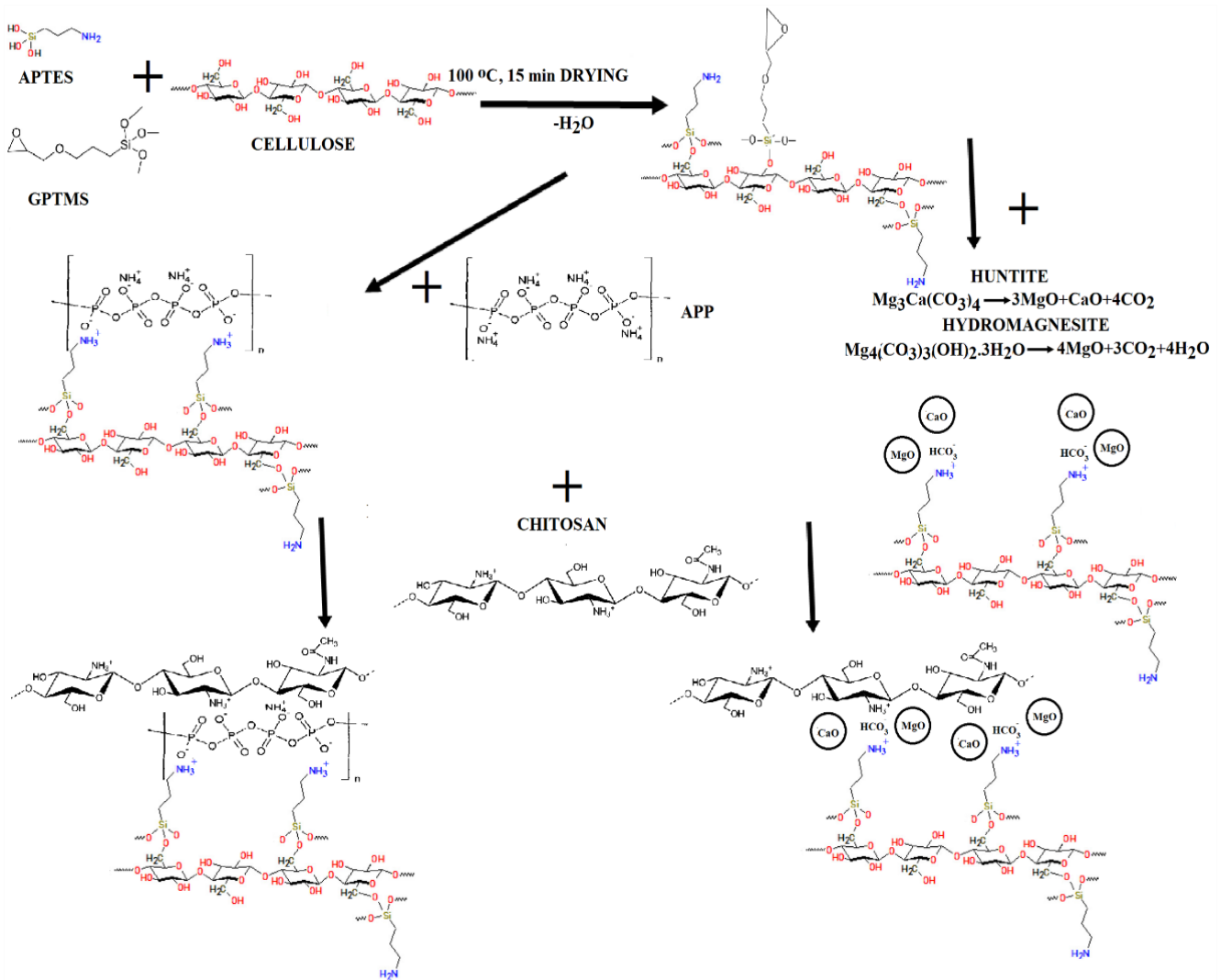
Figure 1. Schematic presentation of interaction of anionic and cationic charged chemicals with cellulose

In the study, experimental parameters were the type of anionic solution, the presence of drying step after every coating and the number of bilayers. The fabrics were dried at 100 °C for 15 min after every dipping process (DE) or only last dipping process (DL). The codes were given as HxDE, HxDL and APxDE, APxDL for coating with HH and APP as anionic layer with x=5, 10 and 15 bilayers and drying (DE code) after every dipping process or drying (DL) only last dipping, respectively.

2.3 Measurement and Characterization

Mineral contents and mean particle size values of HH powders were given in our previous paper [11]. The weight gain of cotton fabrics was designated by measuring the fabric weights before and after LBL assembly. Tensile strength values of fabric samples were measured by tensile testing machine (Tinius Olsen Ltd.) according to ASTM D5035-95 standard (strip method). The yellowness index (E313) and whiteness index (Stensby) were determined by DataColor SpectraFlash 600 spectrophotometer (D65 day light, 10º standard observer). The limited oxygen indexes

(LOI) of samples were analyzed by LOI measurement device (Qualitest Inc., Canada) in accordance with the ASTM D2863 standard. Vertical flame spreading tests (VFT) were applied with face ignition on rectangular samples (50x150 mm2). The short side of the samples was exposed to the flame (20 mm length) for 5 secs. Afterflame time and afterglow time values were determined as explained in ISO 13943 [38]. The images of fabric samples after vertical flame spreading tests were taken. Cone calorimetry test was carried out to charaterize the combustion properties of fabric samples (100mm x 100mm x 0.3mm) under 35 kW/m^2 of irradiative heat flux according to ISO 5660 in horizontal configuration by cone calorimeter (Fire Testing Technology, UK) [39]. Samples were holded with a frame and metallic grid in right position. The total heat release (THR), heat release rate and peak heat release rate (HRR, pkHRR), total smoke release (TSR), CO_2/CO yield, specific extinction area (SEA), time to ignition (TTI), residues at the end of test (wt.%) and mass loss rate (MLR) were evaluated [40]. Thermal analysis of fabric samples was carried out at a heating rate of 20 °C/min in the temperature range of 30-600 °C under

air atmosphere by using DTA-TG machine (Setaram Setsys 1750). The antibacterial activity of the fabric samples was tested as ASTM 2149 standard for S. aureus as Gram-positive organism and E. coli as Gram-negative organism. Bacterial reduction (%) were calculated as Durán et al. 2007 [41]. The surface morphologies of the fabric samples were observed in 1000x and 2000x magnification by using scanning electron microscopy (FESEM, Zeiss Supra 40VP) at acceleration voltage of 20 kV. SEM images of fabric samples were taken before and after vertical flame test (VFT). Their elemental compositions of fabric samples exposed VFT were determined with energy-dispersive X-ray spectroscopy (EDX) before and after 5 washing cycles at 40 ℃ with ECE reference detergent (non-phosphate) as ISO 105 C06. FTIR-ATR spectra of fabric samples were recorded using a Bruker Hyperion 1000 IFS-66/s Infrared Spectrometer with diamond universal ATR accessory and with a resolution of 4 cm^{-1} over a range of 400 to 4000 cm^{-1}.

2. RESULTS AND DISCUSSION

The add-on values, tensile strength, elongation, whiteness and yellowness index values, vertical flame test results (residue amount, after-flame time, after-glow time) and LOI values of the fabric samples are given in Table 1.

3.1 Fabric Characterization

Mass of coating added on the fabrics increased while whiteness of fabric samples was decreasing with the growth of bilayer number, as shown in Table 1 and Figure 2. APP led to further decrease in whiteness and further increase in the mass of coating added on the fabrics compared to HH. Moreover, DE samples possessed lower whiteness and higher add-on values than DL samples. Higher tensile strength of DE samples and lower tensile strength of DL samples in comparison with untreated fabric were illustrated in Figure 3 and Table 1. The tensile strength of all fabric samples increased with the growth of bilayer number. Especially HHxDE samples have the highest tensile strength. Lower elongation of DE samples and

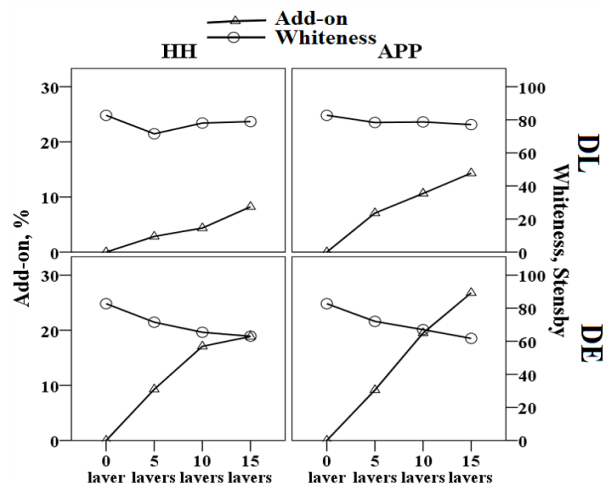higher elongation of DL samples were observed in comparison with untreated fabric.

Figure 2. Add-on and whiteness values of fabric samples with respect to anionic layer type (HH or APP), bilayer numbers and drying conditions (DL or DE)
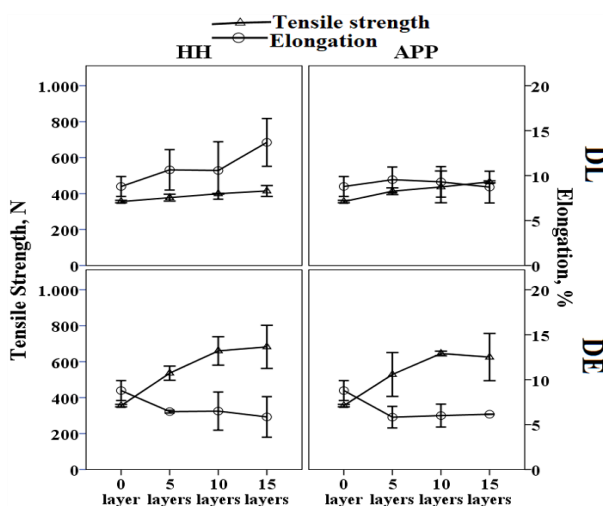

Figure 3. Tensile strength and elongation values with respect to anionic layer type (HH or APP), bilayer numbers and drying conditions (DL or DE)

Table 1. The add on values, tensile strength, elongation, whiteness and yellowness index values, vertical flame test results (residue amount, after-flame time, after-glow time) and LOI values of the fabric samples. *UT-Untreated

| Code | Add-on, % | Yellowness index, E313 | Whiteness index, Stensby | Tensile Strength, N | Elongation, % | Vertical flame test | | | LOI, % |
						Damaged length, mm	After-flame time, s	After-glow time, s	
UT*	-	6.49	82.72	355.60	8.79	120	16	23	17
H5DE	9.9	12.50	71.52	536.00	6.45	120	22	-	18
H10DE	16.3	15.74	65.44	660.00	6.50	120	24	-	19
H15DE	20.4	16.75	63.05	682.50	5.85	120	25	-	19
AP5DE	10.0	11.85	72.02	528.75	5.83	86	18	-	19
AP10DE	20.9	14.35	67.02	645.50	6.00	86	19	-	20
AP15DE	24.6	17.25	61.72	625.50	6.15	90	15	-	22
H5DL	2.4	8.50	78.03	377.60	10.65	120	19	-	18
H10DL	4.1	8.72	78.92	399.20	10.57	120	19	-	18
H15DL	7.9	8.87	78.36	414.75	13.70	120	20	-	18
AP5DL	5.2	8.25	79.54	413.25	9.55	120	24	-	19
AP10DL	9.7	8.59	78.72	437.25	9.30	120	19	-	19
AP15DL	13	9.26	77.09	465.00	8.73	88	13	-	20

3.2 Flame retardancy properties of fabrics

The after-glow time (23s) could be determined for only untreated fabric while all coated fabric samples did not exhibit glow burning behavior, which proved their flame retardant properties. After-flame time of AP code samples decreased from 16s to 15s in comparison with untreated fabric while their damaged length with integrity of char residues have been reducing from 120 mm to 90 mm (Figure 4 h,i,j,m).1 After-flame time of H code samples increased from 16s to 25 s in comparison with untreated fabric, which ascribed slowing of flame spreading on the samples. LOI values of all treated fabrics were increased compared with untreated fabric (17%). LOI values of H code samples (19%) were lower than AP code samples. AP15DE were exerted the highest LOI value (22%) (Figure 5). The results demonstrated their flame retardancy due to high amount of char residue of APP coating and long flame spreading time of HH coating.
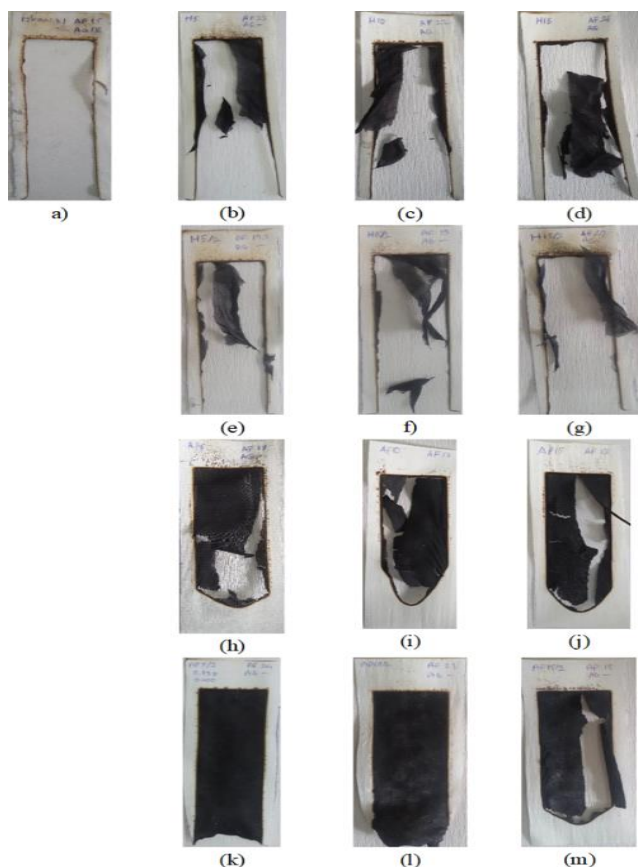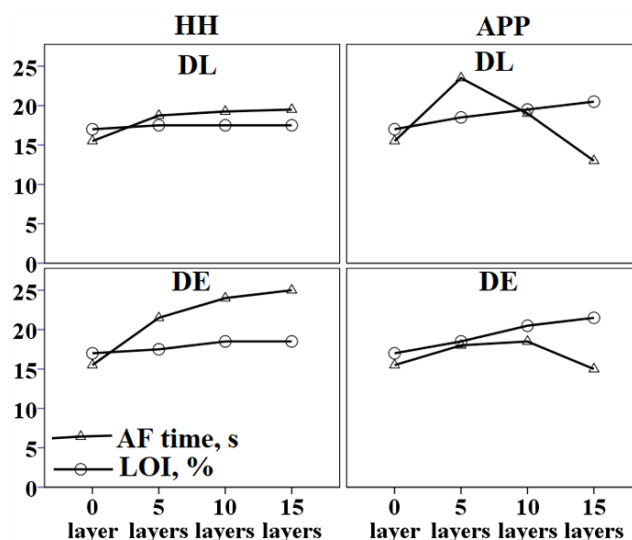

Figure 5. After-flame times and LOI values of samples with respect to anionic layer type (HH or APP), bilayer numbers and drying conditions (DL or DE)

3.3 Cone calorimeter test

Flame retardancy properties of fabric samples were explored by cone calorimeter test. Heat release rate (HRR) and total smoke release (TSR) curves of fabric samples were shown in Figure 6 a) and b). Cone calorimeter test results were depicted in Table 2. It can be observed that the deposition of chitosan, APTES and GPTMS, APP or HH by LBL assembly reduced TTI, pkHRR, pkMLR and TSR values of fabric samples in comparison with untreated fabric. pHRR and MLR values of H15DE and AP15DE samples exhibited further decrease in comparison with H15DL and AP15DL samples. The lowest pHRR (194 kW/m^2) and TSR (18.5 m^2/m^2) values were achieved in H15DE samples while the lowest MLR (11.27 g/(s.m^2)) and residues at the end of test (50%) were succeeded in AP15DE samples. In Figure 7, the images of cone calorimetry test depicted that more residual char amount of AP15DE samples in comparison with untreated fabric and H15DE samples. The samples applied APP in anionic layer acquired lower CO_2/CO yield in comparison with untreated fabric and samples applied HH in anionic layer. Low CO_2/CO yield could be attributed to unyield combustion due to limited difussion of oxygen to pyrolysis area [13,42]. Hence fabric samples used APP or HH in anionic layer exhibited different flame retardancy mechanisms. Reduction on heat release and smoke release attributed flame retardancy (FR) mechanism of samples applied HH in anionic layer. The FR mechanism of the fabric samples used APP as intumescent flame retardant agent was based on high residual char amount, forming a barrier for flame, reducing oxygen diffusion from residual barrier and decelerating of flame progressing. The results were supported by the other flame retardancy test results.

Figure 4. The images of fabric samples exposed to vertical flame test a) UT, b), c), d) HxDE samples with 5, 10 and 15 bilayers, respectively, e), f), g) HxDL samples with 5, 10 and 15 bilayers, respectively, h), i), j) APxDE samples with 5, 10 and 15 bilayers, respectively, k), l), m) APxDL samples with 5, 10 and 15 bilayers, respectively.

Table 2. The cone calorimetry test results

Code	pkHRR [kW/m^2]	THR [MJ/m^2]	pkMLR [g/(s.m^2)]	TSR [m^2/m^2]	CO_2/CO yield	TTI [s]	pkSEA (m^2/kg)	Residues [%]
UT	248	4.2	15.26	146.4	54	11	2407	2
H15DE	194	3.3	13.07	18.5	27	9	2033	3
H15DL	249	2.5	15.00	25.4	20	8	605	1

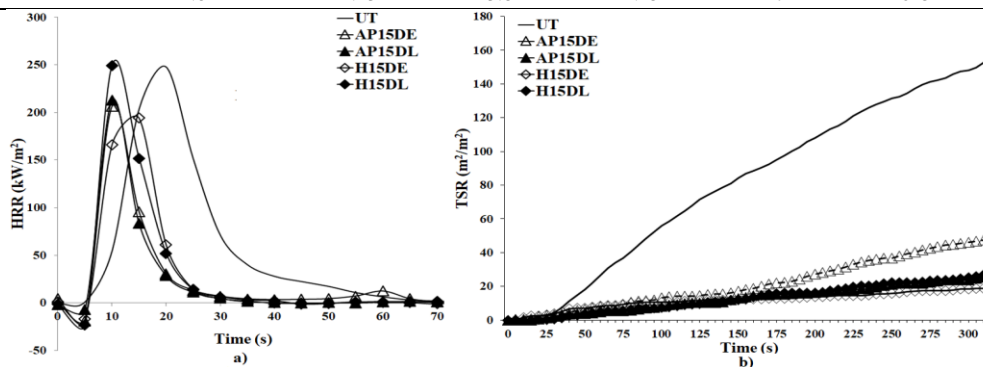| AP15DE | 206 | 2.1 | 11.27 | 45.6 | 2.64 | 8 | 1318 | 50.19 |
| AP15DL | 212 | 1.8 | 14.43 | 23.8 | 2.45 | 7 | 615 | 16.53 |

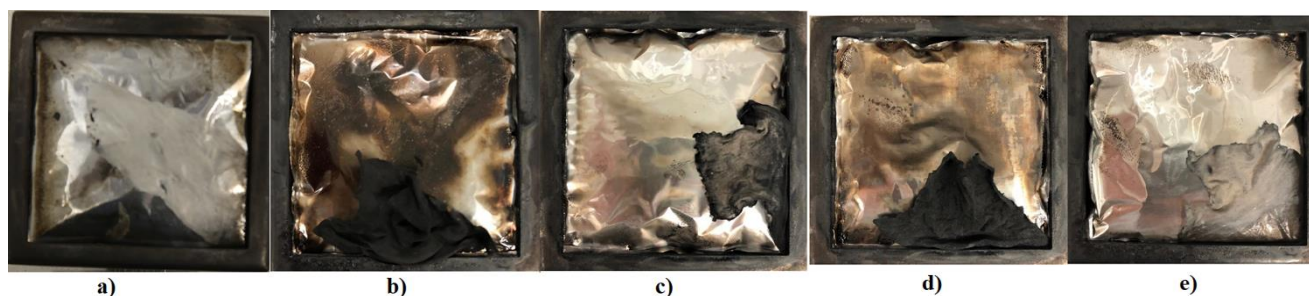**Figure 6.** a) HRR and b) TSR curves of fabric samples

Figure 7. The fabric images after cone calorimetry test a) UT, b) AP15DE, c) H15DE, d) AP15DL, e) H15DL

3.4 Thermogravimetric analysis of fabric samples

The thermal stability of the fabric samples has been investigated by thermogravimetric analysis in air atmosphere. DTG and TG curves of the fabric samples were illustrated in Figure 8 a) and b), respectively and the corresponding datas were summarised in Table 3. Silica was bonded to cellulose by hydrolysis and condensation reactions and then exploited electrostatically interaction with phosphoric acid formed by APP or bicarbonate anions generated by HH. Substantially chitosan as additional carbon source electrostatically collaborated with Cellulose-Silica-APP or Cellulose-Silica-HH to improve FR efficiency of samples (Figure 1). Cationic chitosan in acid solution could be paired with anionic APP solution or HH solution by LBL assembly. Chitosan with nitrogen content and APP with intumescent nature improve the flame retardacy properties of treated materials [6]. Coatings with silica based nanosols could ensure fire protection by forming inorganic barrier. Silica together with nitrogen-based compounds could catalyze the dehydration and carbonization of substrate and decrease the amount of combustible gases.

All samples exhibited two-step thermal degradation processes, where the first step temperature decreased and the second step temperature increased for HxDE, APxDE and APxDL samples in comparison with UT samples. Cotton begins to decompose at 220 ºC ($T_{onset5\%}$) and showed the maximum weight loss rate at 360 ºC (T_{max1}) in the first step, which may be attributed to depolymerization and dehydration of cellulose, formation of aliphatic char. During the second step, the aliphatic char carbonizes into aromatic char and then oxidizes into CO_2 and CO with the

maximum weight loss rate at 495 ºC (T_{max2}) [6]. Lower pyrolysis temperature (T_{max1}) and higher T_{max2} are evident that fabric samples treated LBL show good thermal stability. Especially APxDE samples have lower Tmax1 and higher T_{max2} in comparison with HxDE samples. It was indicated that APP samples had higher thermal stability and higher char residues than HH samples because of the synergistic interaction between phosphorus, nitrogen and silicium atoms in its molecular structure [43]. By introducing the CH-APTES-APP (AP15DE) assembly coating, the fabrics (152 ºC) showed reduced decomposition temperature ($T_{onset5\%}$) compared with untreated fabric (220 ºC). Lower $T_{onset5\%}$ temperature generally could be attributed to thermal degradation of cotton which catalyzed by hydroxyl groups of chitosan and silica [13,44]. APxDE and HxDE exhibited lower pyrolysis temperatures (T_{max1}) in the first step, which is attributable to the catalyzed thermal degradation of cotton in the presence of Si, nitrogen, APP or HH [6]. The growth of bilayer number resulted in a lower pyrolysis temperature and thus higher thermal stability of cotton in the whole degradation process. Because char forming at lower temperatures and volatile species releasing inhibited the further degradation and combustion of cotton at higher temperature [6,13,45]. Hence the second degradation step of AP15DE and H15DE fabric samples (T_{max2}) was postponed to 527 and 516 ºC respectively, dedicating more stable char at higher temperatures in comparison with the uncoated cotton (495 ºC). Final residue amounts of the fabric samples at 600 ºC increased in comparison with UT samples (0.06%). According to char residue datas, the char residue of AP15DE and H15DE were 6.73 and 0.60%, respectively. The char residues of APP and HH samples may be

attributed to the presence of amino and silane groups, benzene rings and phosphate groups or calcium and magnesium oxides. All these results indicated that thermal stability of LBL treated fabric samples improved the by

supporting the char formation and preventing the production of volatile species.

Table 3. DTA-TG datas for untreated and treated fabric samples. $T_{onset5\%}$: Initial decomposition temperature (for 5% weight loss) [40]. T_{max}: Maximum weight loss temperature (from DTG curves)

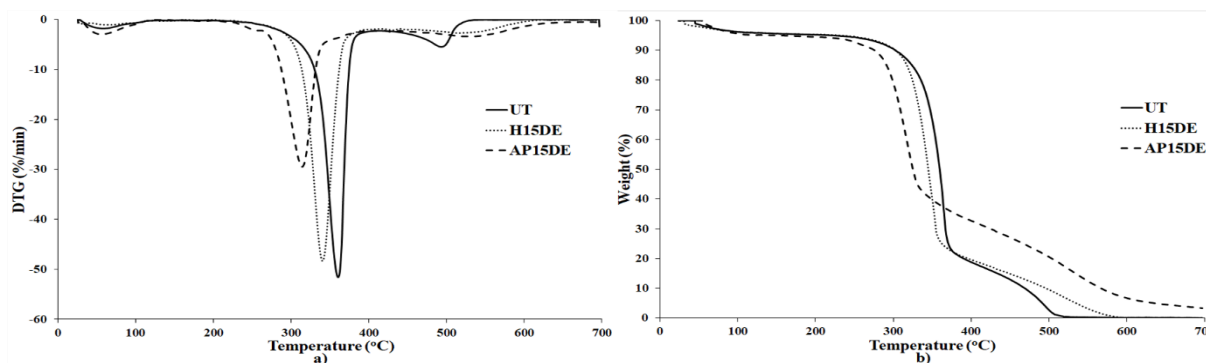| Code	$T_{onset5\%}$, °C	T_{max1}, °C	T_{max2}, °C	Residue at T_{max1}, %	Residue at T_{max2}, %	Residue at 600 °C, %
UT	220	360	495	48	5	0.06
AP5DE	261	335	521	55	9	1.25
AP10DE	249	330	536	61	14	6.00
AP15DE	152	314	527	61	16	6.73
H5DE	276	358	520	50	6	0.25
H10DE	281	346	508	55	8	0.32
H15DE	232	340	516	52	7	0.60

Figure 8. a) DTG and b) TG graphs of fabric samples

3.5 Antibacterial properties of fabric samples

The bacterial reduction for E. coli and S. aureus was examined in H15DE and AP15DE samples. It was found from Figure 9 and 10 that AP15DE samples had high bacterial reduction, 100% and 98% against *E.coli* and *S. aureus*, respectively. The antibacterial activity of APP did not previously study in the literature. Nitrogen and phosphate contents of APP attributed to their antibacterial activity. An effective bacteriostatic effect stem from cationic ammonium and polyphosphates in its structure [46, 47]. Amino groups through ionic interaction could absorbed on the anionic cell walls of bacteria [48]. The bacterial reduction of H15DE sample against to *S. aureus* reached to 93% due to the presence of CaO and MgO ensuring superoxide forming in HH powder while the bacterial reduction against to *E.coli* was 61%. Rough coating with HH powder observed SEM images could provide higher specific area and thus efficient contact and interaction between HH powder and S. aureus (Figure 11). Antibacterial activity of MgO and CaO could be ascribed to form of superoxide on material surface [11,49]. APP or HH in outer layer of fabric samples was in charge of bacteristatic activity [50].
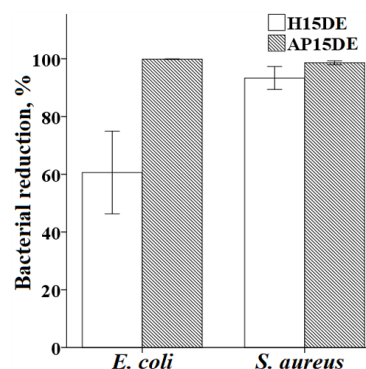

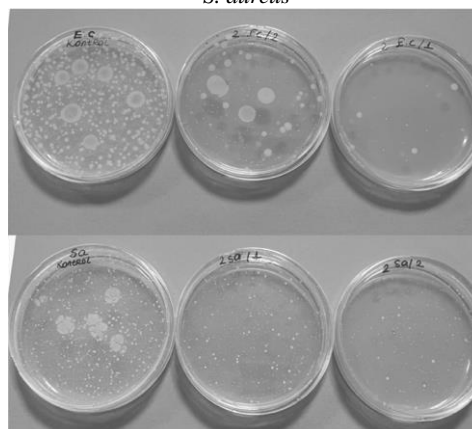**Figure 9.** Bacterial reduction of fabric samples againsts *E. coli* and *S. aureus*

Figure 10. Images of bacterial reduction test a) UT, b) H15DE, c) AP15DE against to *E.coli* and d) UT, e) H15DE, f) AP15DE against to *S.aureus*

3.6 SEM-EDS and FTIR Analyses

The SEM images in Figure 11 showed the surface structure of the fabric samples. These micrographs reveal that all fibers treated LBL with HH in anionic layer exhibited superficial and rough coating and no bridging between fibers while HxDL samples displayed the presence of particulate matters on the surface with the growth of bilayer numbers. Aggregation of HH powder was observed in HxDL samples while regular film form was exhibited in HxDE samples with attribution based on drying processes. The coating on APxDE samples was filling between fiber with continuous and denser layer while some cracks were observed on the coating on APxDL samples. Figure 12 illustrated the SEM images of UT, AP15DE and H15DE samples after VFT and washing cycles+VFT. The treated samples protected integrity after VFT and washing cycles+VFT. Especially AP15DE sample exhibited better contiunity after VFT, which supported by photos and residual amounts in VFT and cone calorimetry analysis.
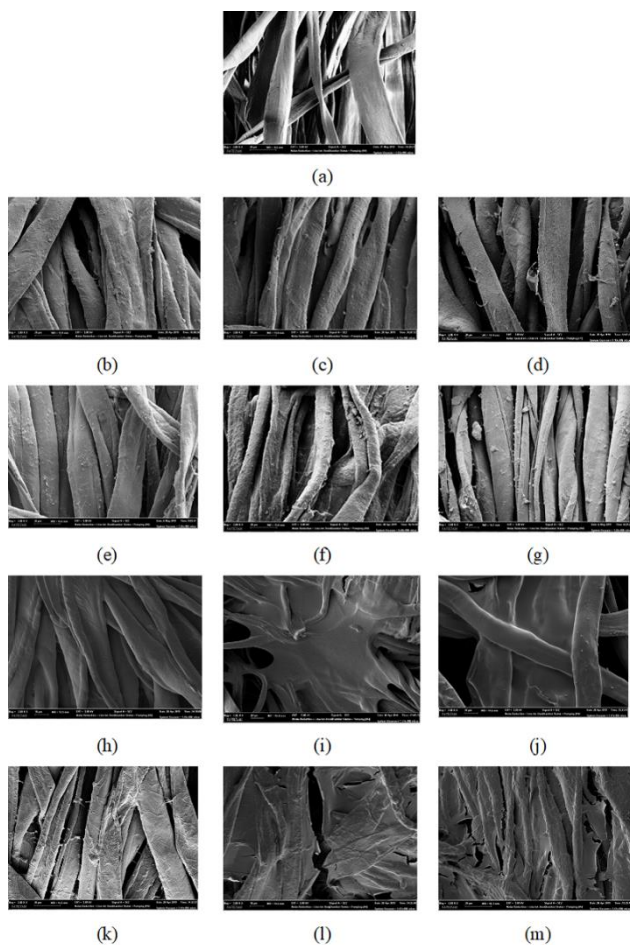

Figure 11. SEM images of fabric samples a) UT, b)H5DE, c)H10DE, d)H15DE, e)H5DL, f)H10DL, g)H15DL, h)AP5DE, i)AP10DE, j)AP15DE, k)AP5DL, l)AP10DL, m)AP15DL
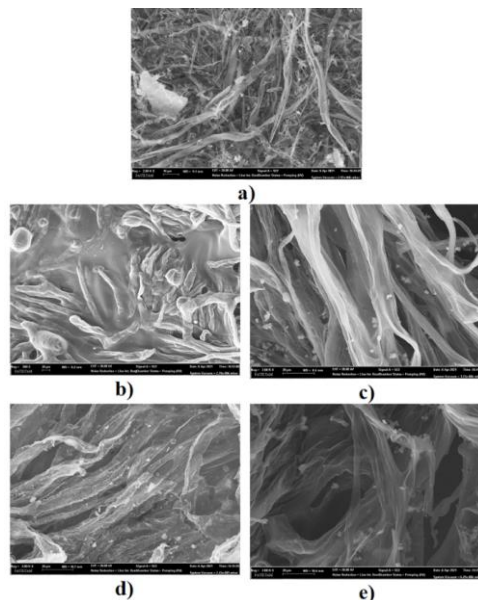

Figure 12. SEM images After washing cycles and vertical flame test a) UT after VFT b) AP15DE after VFT c) AP15DE after washing cycles and VFT d) H15DE after VFT e) H15DE after washing cycles and VFT

To confirm the flame-retardant composition on fabric samples, the presence and durability of the elements on treated fabric samples were analyzed by SEM-EDS techniques. Elemental analysis results of AP15DE and H15DE samples after VFT and washing cycles+VFT were given in Figure 13. The result showed that the samples contained silicium element from APTES and GPTMS and nitrogen element from APTES, chitosan and APP. It was also confirmed the presence of Ca and Mg elements in H code samples and the presence of phosphate in AP code samples. The flame retardant efficiency of especially APxDE samples could be attributed to high content of P, N, and Si. The results proved the durability of coated samples to washing.

The chemical structures of untreated and LBL treated fabrics have been evaluated by FTIR-ATR spectra. As shown in Figure 14, all fabric samples showed wide peak between 3000 and 3600 cm^{-1}, characteristic signals between 1035 and 1160 cm^{-1}, peaks about 2900 cm^{-1}, 1635 cm^{-1}, 1428 cm^{-1}, 1361 cm^{-1} and 1053 cm^{-1} ascribed to the stretching at OH groups, the C-O-C of cellulose backbone, stretching vibration at C-H groups in alkyl chains, bending at O-H groups of adsorbed water, deformation vibration at -CH_2-, bending vibration of C-H groups and stretching vibration of C-O-C groups which these peaks were stems from cellulose nature [6,13,25]. The signals between 1000 and 1100 cm^{-1} in all fabrics were ascribed to Si–O–Si bond asymmetric stretching vibration, which indicated the presence of silica network, and overlapped with inherent peaks of cellulose [51,52]. Chitosan depicted similar peaks to cellulose and also wide peak at 3333 cm^{-1} attributed to stretching vibration of N-H groups. The peak at 1740 cm^{-1} contributed by stretching vibration of carbonyl group (C=O) [53]. Furthermore, APP, HH and APTES in coating layer demonstrated characteristic peaks on spectras of fabric samples in Figure 14. The band at 1440 cm^{-1} corresponds to the bending vibration of CH_2 groups next to the nitrogen atom [54]. Meanwhile a peak at 1532 cm^{-1}

contributed by bending vibration of –NH2 groups from APTES and chitosan appeared in LBL treated fabrics. The peak at 1232 cm^{-1} ascribed to stretching vibration of P-O-aryl proved the presence of phosphate on AP code samples, which overlapped Si-C band at 1200 cm^{-1} for all LBL treated fabric samples [6,25,55]. It was determined that a peak at 1040 cm^{-1} ascribed to stretching vibration of P-O-C from AP15DE overlapped with peak at 1052 cm^{-1} ascribed to stretching vibration of C-O-C from cellulose, which was supported by Pan et al. 2015 [30]. Two peaks for H15DE at

1538 cm^{-1} and 1508 cm^{-1} were ascribed to asymmetric bands of CO_3^{-2} groups of HH. The peak at 1538 cm^{-1} overlapped with bending vibration of –NH$_2$ groups at 1532 cm^{-1} from APTES and chitosan. Furthermore, two peaks at 870 ve 891 cm^{-1} were ascribed to carbonate ligand from HH [11,16,56]. Overall, the FTIR-ATR spectra confirmed that chitosan, APTES and APP or HH were successfully applied to fabric samples.
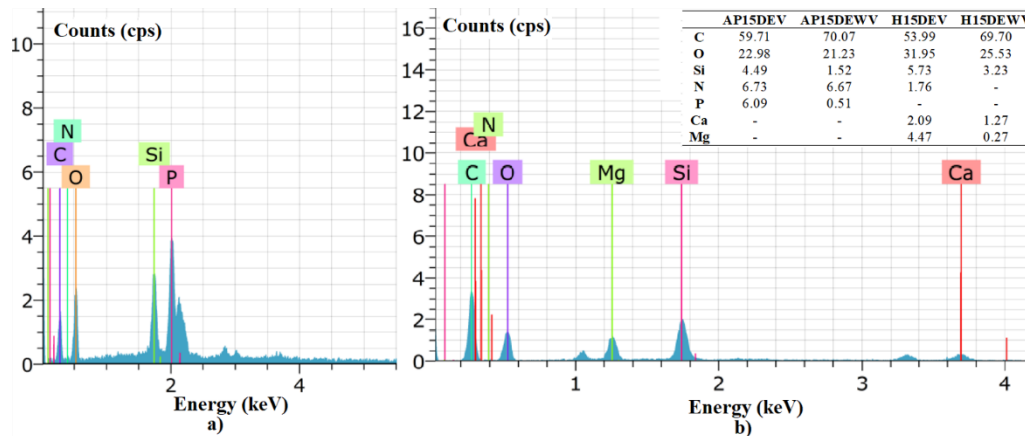

	AP15DEV	AP15DEWV	H15DEV	H15DEWV
C	59.71	70.07	53.99	69.70
O	22.98	21.23	31.95	25.53
Si	4.49	1.52	5.73	3.23
N	6.73	6.67	1.76	-
P	6.09	0.51	-	-
Ca	-	-	2.09	1.27
Mg	-	-	4.47	0.27

Figure 13. The elemental composition of the fabric samples by EDS analysis (gravimetric, %) after vertical flame test (V) and washing cycles (W) a)AP15DEV and b) H15DEV samples
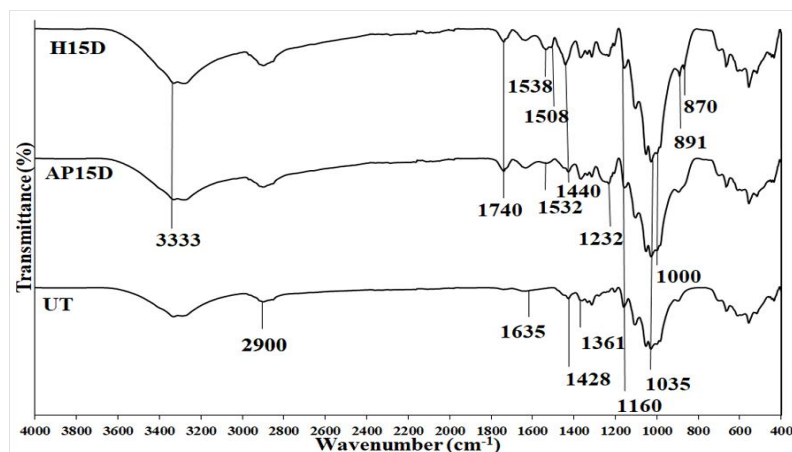

Figure 14. FTIR spectrum for UT, AP15DE and H15DE samples.

3. CONCLUSION

In this article, we have demonstrated that successful fabrication of flame retardant, smoke supressed and antibacterial cotton fabric with application of chitosan, and APTES as cationic layer and APP or HH as anionic layer by LBL assembly. It was investigated the effect of bilayer numbers (5, 10 and 15 bilayers), anionic layer type (APP or HH) and drying conditions (DE or DL) on multifunctionality of cotton fabrics. LBL treated fabrics displayed different behaviors in terms of fabric characteristics and hence, reflected on their flame retardant and antibacterial properties. LBL treated fabric samples revealed some increase in LOI values (i.e., from 17% to 22% for AP15DE and 19% for

H15DE), get longer AF time (from 16s to 25s for H15DE) and shorter damaged length (from 12 cm to 9 cm for AP15DE) in vertical flame test, significant decrease in pHRR and TSR value (from 248 to 194 kW/m^2 and from 146 to 18.5 m^2/m^2 for H15D) in cone calorimetry test and significant increase residue at 600 °C (6.73% residue for AP15DE) in DTA-TG analysis in comparison with untreated fabric. It was concluded that the flame retardancy mechanism of AP15DE samples as intumescent flame retardant agent was based on increasing char amount, which formed a barrier for flame, decreased oxygen transfer, and decelerating of flame progressing while the mechanism of H15DE samples was resulted from long afterflame time and decreasing smoke density and heat release. AP15DE imparted high

bacteriostatic reduction agaits two bacterias while H15DE exhibited high bacterial reduction against only *S. aureus*. In conclusion, it was proved the antibacterial and flame retardancy properties of the coated fabrics with HH or APP as anionic layer and chitosan and silane based nanosols as cationic layer by LBL assembly. There was some researches on the using of APP for LBL assembly on cotton fabric while the using of HH solution as aninonic layer for LBL assembly on cotton fabric were firstly studied in literature. Their antibacterial and flame retardancy performance was compared and they were proposed their usage for medical, industrial, home and military textiles.

REFERENCES

1. Li, S., Lin, X., Liu, Y., Li, R., Ren, X., & Huang, T. S. 2019. Phosphorus-nitrogen-silicon-based assembly multilayer coating for the preparation of flame retardant and antimicrobial cotton fabric. *Cellulose*, 26(6), 4213-4223.

2. Onar Camlibel N, Topcu H. 2021. Flame retardant cotton fabric modified with silica nanosols containing huntite–hydromagnesite grafted with GPTMS and VTES. *The Journal of The Textile Institute*, 112(7), 1129-1143.

3. Atay, H. Y., & Engin, B. 2019. Use of glass fibers and glass spheres to improve mechanical properties of huntite and hydromagnesite reinforced flame retardant composites. *Revista Română de Materiale/Romanian Journal of Materials*, 49(4), 468-474.

4. Hollingbery, L. A., & Hull, T. R. 2010. The thermal decomposition of huntite and hydromagnesite—a review. Thermochimica Acta, 509(1-2), 1-11.

5. Kangal, O., Kökkılıç, O., & Burat, F. 2009. Production of huntite and hydromagnesite with flame retardant featured by flotation. *Mining, Metallurgy & Exploration*, 26(2), 109-113.

6. Fang, F., Zhang, X., Meng, Y., Gu, Z., Bao, C., Ding, X., ... & Tian, X. 2015. Intumescent flame retardant coatings on cotton fabric of chitosan and ammonium polyphosphate via layer-by-layer assembly. *Surface and Coatings Technology*, 262, 9-14.

7. Wang, X., Romero, M. Q., Zhang, X. Q., Wang, R., & Wang, D. Y. 2015. Intumescent multilayer hybrid coating for flame retardant cotton fabrics based on layer-by-layer assembly and sol–gel process. *RSC advances*, 5(14), 10647-10655.

8. Devaux, E., Rochery, M., & Bourbigot, S. 2002. Polyurethane/clay and polyurethane/POSS nanocomposites as flame retarded coating for polyester and cotton fabrics. *Fire and Materials*, 26(4-5), 149-154.

9. Grancaric, A. M., Colleoni, C., Guido, E., Botteri, L., & Rosace, G. 2017. Thermal behaviour and flame retardancy of monoethanolamine-doped sol-gel coatings of cotton fabric. *Progress in Organic Coatings*, 103, 174-181.

10. Spontón, M., Ronda, J. C., Galià, M., & Cádiz, V. 2009. Development of flame retardant phosphorus-and silicon-containing polybenzoxazines. *Polymer degradation and stability*, 94(2), 145-150.

11. Camlibel, N. O., Avinc, O., Arik, B., Yavas, A., & Yakin, I. 2019. The effects of huntite–hydromagnesite inclusion in acrylate-based polymer paste coating process on some textile functional performance properties of cotton fabric. *Cellulose*, 26(2), 1367-1381.

12. Alongi, J., Carosio, F., & Malucelli, G. 2012. Influence of ammonium polyphosphate-/poly (acrylic acid)-based layer by layer architectures on the char formation in cotton, polyester and their blends. *Polymer Degradation and Stability*, 97(9), 1644-1653.

13. Carosio, F., Alongi, J., & Malucelli, G. 2012. Layer by layer ammonium polyphosphate-based coatings for flame retardancy of polyester–cotton blends. *Carbohydrate Polymers*, 88(4), 1460-1469.

14. Mateos, A. J., Cain, A. A., & Grunlan, J. C. 2014. Large-scale continuous immersion system for layer-by-layer deposition of flame retardant and conductive nanocoatings on fabric. *Industrial & Engineering Chemistry Research*, 53(15), 6409-6416.

15. Jimenez, M., Guin, T., Bellayer, S., Dupretz, R., Bourbigot, S., & Grunlan, J. C. 2016. Microintumescent mechanism of flame-retardant water-based chitosan–ammonium polyphosphate multilayer nanocoating on cotton fabric. *Journal of Applied Polymer Science*, 133(32).

16. Zhang, T., Yan, H., Peng, M., Wang, L., Ding, H., & Fang, Z. 2013. Construction of flame retardant nanocoating on ramie fabric via layer-by-layer assembly of carbon nanotube and ammonium polyphosphate. *Nanoscale*, 5(7), 3013-3021.

17. Wattanatanom, W., Churuchinda, S., & Potiyaraj, P. 2017. Intumescent flame retardant finishing of polyester fabrics via the layer-by-layer assembly technique. *International Journal of Clothing Science and Technology,* 29(1), 96-105.

18. Li, H., & Peng, L. 2015. Antimicrobial and antioxidant surface modification of cellulose fibers using layer-by-layer deposition of chitosan and lignosulfonates. *Carbohydrate polymers*, 124, 35-42.

19. Shirvan, A. R., Nejad, N. H., & Bashari, A. 2014. Antibacterial finishing of cotton fabric via the chitosan/TPP self-assembled nano layers. *Fibers and Polymers*, 15(9), 1908-1914.

20. Joshi, M., Khanna, R., Shekhar, R., & Jha, K. 2011. Chitosan nanocoating on cotton textile substrate using layer-by-layer self-assembly technique. *Journal of Applied Polymer Science*, 119(5), 2793-2799.

21. Ali, S. W., Joshi, M., & Rajendran, S. 2011. Novel, Self-Assembled Antimicrobial Textile Coating Containing Chitosan Nanoparticles. *Aatcc Review*, 11(5).

22. Gadkari, R. R., Ali, S. W., Joshi, M., Rajendran, S., Das, A., & Alagirusamy, R. 2020. Leveraging antibacterial efficacy of silver loaded chitosan nanoparticles on layer-by-layer self-assembled coated cotton fabric. *International Journal of Biological Macromolecules*, 162, 548-560.

23. Saini S, Gupta A, Singh N, Sheikh J. Functionalization of linen fabric using layer by layer treatment with chitosan and green tea extract. J. Ind. Eng. Chem. 2020; 82: 138-143.

24. Leistner, M., Abu-Odeh, A. A., Rohmer, S. C., & Grunlan, J. C. 2015. Water-based chitosan/melamine polyphosphate multilayer nanocoating that extinguishes fire on polyester-cotton fabric. *Carbohydrate polymers*, 130, 227-232.

25. Liu, Y., Wang, Q. Q., Jiang, Z. M., Zhang, C. J., Li, Z. F., Chen, H. Q., & Zhu, P. 2018. Effect of chitosan on the fire retardancy and thermal degradation properties of coated cotton fabrics with sodium phytate and APTES by LBL assembly. *Journal of analytical and applied pyrolysis*, 135, 289-298.

26. Yu, X., Pan, Y., Wang, D., Yuan, B., Song, L., & Hu, Y. 2017. Fabrication and properties of biobased layer-by-layer coated ramie fabric-reinforced unsaturated polyester resin composites. *Industrial & Engineering Chemistry Research*, 56(16), 4758-4767.

27. Carosio, F., Laufer, G., Alongi, J., Camino, G., & Grunlan, J. C. 2011. Layer-by-layer assembly of silica-based flame retardant thin

film on PET fabric. *Polymer Degradation and Stability*, 96(5), 745-750.

28. Laufer, G., Carosio, F., Martinez, R., Camino, G., & Grunlan, J. C. 2011. Growth and fire resistance of colloidal silica-polyelectrolyte thin film assemblies. *Journal of colloid and interface science*, 356(1), 69-77.

29. Pan, H., Song, L., Ma, L., Pan, Y., Liew, K. M., & Hu, Y. 2014. Layer-by-layer assembled thin films based on fully biobased polysaccharides: chitosan and phosphorylated cellulose for flame-retardant cotton fabric. *Cellulose*, 21(4), 2995-3006.

30. Pan, H., Wang, W., Pan, Y., Song, L., Hu, Y., & Liew, K. M. 2015. Formation of self-extinguishing flame retardant biobased coating on cotton fabrics via Layer-by-Layer assembly of chitin derivatives. *Carbohydrate polymers*, 115, 516-524.

31. Pan, Y., Wang, W., Pan, H., Zhan, J., & Hu, Y. 2016. Fabrication of montmorillonite and titanate nanotube based coatings via layer-by-layer self-assembly method to enhance the thermal stability, flame retardancy and ultraviolet protection of polyethylene terephthalate (PET) fabric. *RSC advances*, 6(59), 53625-53634.

32. Li, Y., Wang, B., Sui, X., Xie, R., Xu, H., Zhang, L., ... & Mao, Z. 2018. Durable flame retardant and antibacterial finishing on cotton fabrics with cyclotriphosphazene/polydopamine/silver nanoparticles hybrid coatings. *Applied Surface Science*, 435, 1337-1343.

33. Li, P., Wang, B., Liu, Y. Y., Xu, Y. J., Jiang, Z. M., Dong, C. H., ... & Zhu, P. 2020. Fully bio-based coating from chitosan and phytate for fire-safety and antibacterial cotton fabrics. *Carbohydrate Polymers*, 237, 116173.

34. Nine, M. J., Tran, D. N., ElMekawy, A., & Losic, D. 2017. Interlayer growth of borates for highly adhesive graphene coatings with enhanced abrasion resistance, fire-retardant and antibacterial ability. *Carbon*, 117, 252-262.

35. Safi, K., Kant, K., Bramhecha, I., Mathur, P., & Sheikh, J. 2020. Multifunctional modification of cotton using layer-by-layer finishing with chitosan, sodium lignin sulphonate and boric acid. *International Journal of Biological Macromolecules*, 158, 903-910.

36. Fang, F., Xiao, D., Zhang, X., Meng, Y., Cheng, C., Bao, C., ... & Tian, X. 2015. Construction of intumescent flame retardant and antimicrobial coating on cotton fabric via layer-by-layer assembly technology. *Surface and Coatings Technology*, 276, 726-734.

37. Fang, F., Chen, X., Zhang, X., Cheng, C., Xiao, D., Meng, Y., ... & Tian, X. 2016. Environmentally friendly assembly multilayer coating for flame retardant and antimicrobial cotton fabric. *Progress in Organic Coatings*, 90, 258-266.

38. Alongi, J., Cuttica, F., Carosio, F., & Bourbigot, S. 2015. How much the fabric grammage may affect cotton combustion?. *Cellulose*, 22(5), 3477-3489.

39. Tata, J., Alongi, J., Carosio, F., & Frache, A. 2011. Optimization of the procedure to burn textile fabrics by cone calorimeter: Part I. Combustion behavior of polyester. *Fire and materials*, 35(6), 397-409.

40. Alongi, J., Ciobanu, M., Tata, J., Carosio, F., & Malucelli, G. 2011. Thermal stability and flame retardancy of polyester, cotton, and relative blend textile fabrics subjected to sol–gel treatments. *Journal of Applied Polymer Science*, 119(4), 1961-1969.

41. Durán, N., Marcato, P. D., De Souza, G. I., Alves, O. L., & Esposito, E. 2007. Antibacterial effect of silver nanoparticles produced by fungal process on textile fabrics and their effluent treatment. *Journal of biomedical nanotechnology*, 3(2), 203-208.

42. Kandare, E., Kandola, B. K., Price, D., Nazare, S., & Horrocks, R. A. 2008. Study of the thermal decomposition of flame-retarded unsaturated polyester resins by thermogravimetric analysis and Py-GC/MS. *Polymer Degradation and Stability*, 93(11), 1996-2006.

43. Zhao, P., Li, X., Zhang, M., Liu, S., Liang, W., & Liu, Y. 2014. Highly flame-retarding cotton fabrics with a novel phosphorus/nitrogen intumescent flame retardant. *Korean Journal of Chemical Engineering*, 31(9), 1592-1597.

44. Xie, W., Gao, Z., Pan, W. P., Hunter, D., Singh, A., & Vaia, R. 2001. Thermal degradation chemistry of alkyl quaternary ammonium montmorillonite. *Chemistry of materials*, 13(9), 2979-2990.

45. Horrocks, A. R. 2011. Flame retardant challenges for textiles and fibres: New chemistry versus innovatory solutions. *Polymer Degradation and Stability*, 96(3), 377-392.

46. Wang, L., Wen, X., Zhang, X., Yuan, S., Xu, Q., Fu, F., ... & Liu, X. 2021. Durable antimicrobial cotton fabric fabricated by carboxymethyl chitosan and quaternary ammonium salts. *Cellulose*, 28(9), 5867-5879.

47. Lee TS, Kim SJ, Chang DS. 1988. Bacteriostatic effect of condensed phosphate on the growth of bacteria. *Korean Journal of Fisheries and Aquatic Sciences*, 21(2), 97-104.

48. Liu, J., Dong, C., Wei, D., Zhang, Z., Xie, W., Li, Q., & Lu, Z. 2019. Multifunctional antibacterial and hydrophobic cotton fabrics treated with cyclic polysiloxane quaternary ammonium salt. *Fibers and Polymers*, 20(7), 1368-1374.

49. Yamamoto, O., Ohira, T., Alvarez, K., & Fukuda, M. 2010. Antibacterial characteristics of CaCO3–MgO composites. *Materials Science and Engineering: B*, 173(1-3), 208-212..

50. Pérez, O. P., & Matte, Y. C. 2017. Synthesis, characterization, and assessment of the antimicrobial activity of MgO–calcium alginate porous beads. *Tecnia*, 26(2), 7-13.

51. Cireli, A., Onar, N., Ebeoglugil, M. F., Kayatekin, I., Kutlu, B., Culha, O., & Celik, E. 2007. Development of flame retardancy properties of new halogen-free phosphorous doped SiO2 thin films on fabrics. *Journal of Applied Polymer Science*, 105(6), 3748-3756.

52. Onar Ni, Mete G. 2016. Development of water repellent cotton fabric with application of ZnO, Al$_2$O$_3$, TiO$_2$ and ZrO$_2$ nanoparticles modified with ormosils. *Textile and Apparel*, 26(3), 295-302.

53. Jiang, C., Liu, W., Sun, Y., Liu, C., Yang, M., & Wang, Z. 2019. Fabrication of durable superhydrophobic and superoleophilic cotton fabric with fluorinated silica sol via sol–gel process. *Journal of Applied Polymer Science*, 136(4), 47005.

54. Mosnáčková, K., Chehimi, M. M., Fedorko, P., & Omastová, M. 2013. Polyamide grafted with polypyrrole: formation, properties, and stability. *Chemical Papers*, 67(8), 979-994.

55. Škoc, M. S., Macan, J., & Pezelj, E. 2014. Modification of polyurethane-coated fabrics by sol–gel thin films. *Journal of Applied Polymer Science*, 131(4).

56. Şen, F., Madakbaş, S., & Kahraman, M. V. 2014. Preparation and characterization of polyaniline/Turkish Huntite-hydromagnesite composites. *Polymer composites*, 35(3), 456-460.